Clim Dyn (2016) 47:2059–2069
DOI 10.1007/s00382-015-2950-1

The effect of the East Atlantic pattern on the precipitation $\delta^{18}O$-NAO relationship in Europe

L. Comas-Bru[1] · F. McDermott[1,2] · M. Werner[3]

Received: 16 July 2015 / Accepted: 11 December 2015 / Published online: 14 January 2016
© Springer-Verlag Berlin Heidelberg 2016

Abstract The North Atlantic Oscillation (NAO) is known to influence precipitation $\delta^{18}O$ ($\delta^{18}O_p$) through its control on air temperature and on the trajectory of the westerly winds that carry moisture onto Europe during boreal winters. Hence, paleoclimate studies seeking to reconstruct the NAO can exploit the $\delta^{18}O$ signal that is commonly preserved in natural archives such as stalagmites, ice cores, tree rings and lake sediments. However, such reconstructions should consider the uncertainties that arise from non-stationarities in the $\delta^{18}O_p$-NAO relationship. Here, new insights into the causes of these temporal non-stationarities are presented for the European region using both observations (GNIP database) and the output of an isotope-enabled general circulation model (ECHAM5-wiso). The results show that, although the East Atlantic (EA) pattern is generally uncorrelated to $\delta^{18}O_p$ during the instrumental period, its polarity affects the $\delta^{18}O_p$-NAO relationship. Non-stationarities in this relationship result from spatial shifts of the $\delta^{18}O_p$-NAO correlated areas as a consequence of different NAO/EA combinations. These shifts are consistent with those reported previously for NAO-winter climate variables and the resulting non-stationarities mean that $\delta^{18}O$-based NAO reconstructions could be compromised if the balance of positive and negative NAO/EA states differs substantially in a calibration period compared with the period of interest in the past. The same approach has been followed to assess the relationships between $\delta^{18}O_p$ and both winter total precipitation and winter mean surface air temperature, with similar results. Crucially, this study also identifies regions within Europe where temporal changes in the NAO, air temperature and precipitation can be more robustly reconstructed using $\delta^{18}O$ time series from natural archives, irrespective of concomitant changes in the EA.

Keywords Precipitation $\delta^{18}O$ · North Atlantic Oscillation · East Atlantic pattern · GNIP database · ECHAM5-wiso model

1 Introduction

The control exerted by large scale atmospheric circulation modes on the oxygen isotopic composition of precipitation ($\delta^{18}O_p$) has been utilised to infer past atmospheric circulation states using proxies that capture $\delta^{18}O$ at a wide range of locations (e.g. Smith and Hollander 1999; Feng et al. 2007; Fischer and Mattey 2012). Such reconstructions typically rely on the oxygen isotopic composition of terrestrial archives such as ice-cores, tree rings, speleothems and lacustrine carbonates (Jones et al. 2009) and are underpinned by assumptions about the links between atmospheric circulation modes and the ocean source regions of atmospheric vapour and its transport paths (e.g. Lawrence

Electronic supplementary material The online version of this article (doi:10.1007/s00382-015-2950-1) contains supplementary material, which is available to authorized users.

This work was funded by Science Foundation Ireland through its "Research Frontiers Programme" (10/RFP/GEO2747).

✉ L. Comas-Bru
laia.comasbru@ucd.ie

[1] School of Earth Sciences, University College Dublin, Belfield, Dublin 4, Ireland

[2] UCD Earth Institute, University College Dublin, Belfield, Dublin 4, Ireland

[3] Division Climate Science - Paleoclimate Dynamics, Helmholtz Centre for Polar and Marine Research, Alfred Wegener Institute, Bussestr. 24, 27570 Bremerhaven, Germany

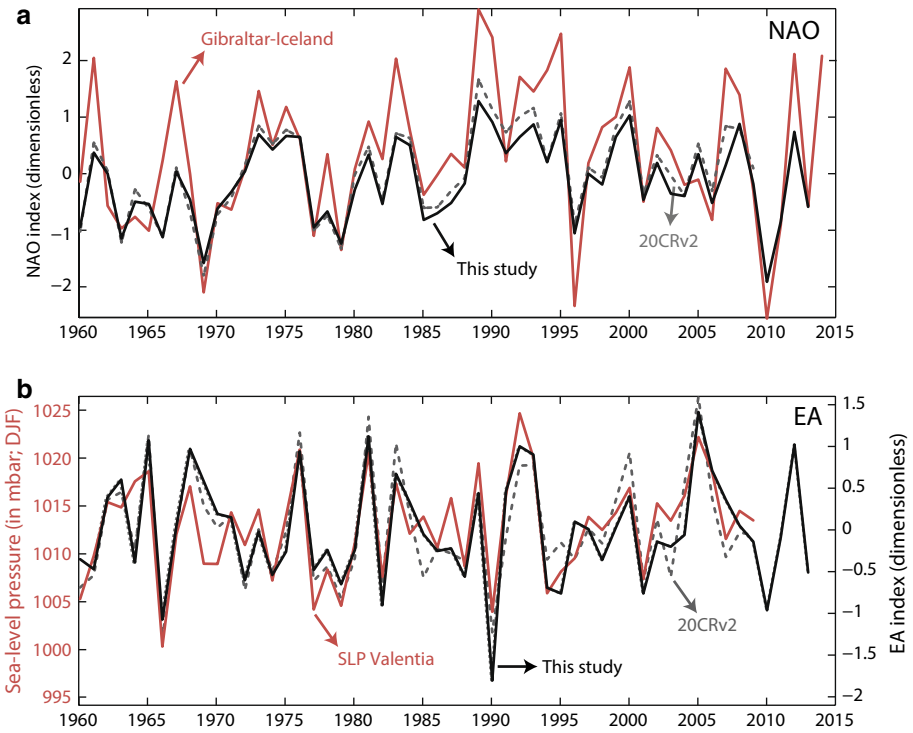

Fig. 1 Time series of the NAO and EA indices. **a** Instrumental NAO index using Gibraltar and SW Iceland stations (*red solid line*; Jones et al. 1997), PC-based NAO index using the 20CRv2 reanalysis dataset (Compo et al. 2011) as used in Comas-Bru and McDermott (2014, *dashed grey line*), and the PC-based NAO index used in this study (*black solid line*). **b** mean winter (DJF) SLP data from Valentia Observatory (in mbar; Ireland) used to derive an instrumental EA index as in Moore and Renfrew (2012, *red solid line*), PC-based EA index using the 20CRv2 reanalysis dataset (Compo et al. 2011) as in Comas-Bru and McDermott (2014, *dashed grey line*), and the PC-based EA index used in this study (*black solid line*). The indices used here (*solid black lines*) are calculated using ERA40 (Uppala et al. 2005) and ERAinterim (Dee et al. 2011) data for the periods December 1957 to February 1979 and December 1979 to February 2013, respectively. Each winter mean is ascribed to the year of January (i.e. Dec 1981 to Feb 1982 mean is reported as 1982) following the common definition for the NAO index (Hurrell 1995)

et al. 1982; Friedman et al. 2002; Baldini et al. 2010; Liu et al. 2010, 2013).

However, since $\delta^{18}O_p$ data are available for the last few decades only and are not spatially or temporally coherent (International Atomic Energy Agency's Global Network of Isotopes in Precipitation, GNIP; IAEA/WMO 2015), palaeoclimate reconstructions are typically based on the assumption of long term stationarity of the influence of the atmospheric teleconnection pattern of interest on $\delta^{18}O_p$, derived from linear relationships between $\delta^{18}O_p$ and the proxy records $\delta^{18}O$ for some overlapping calibration period.

In the N. Atlantic/ European region, substantial efforts have been made to reconstruct past North Atlantic Oscillation (NAO) states, the main driver of European winter climate variability (Hurrell 1995; Hurrell et al. 1981; Wanner et al. 2001), in order to provide the necessary perspective to assess its long-term variability, and to evaluate the potential impact of anthropogenic climate change on the NAO (Luterbacher et al. 2002; Trouet et al. 2009).

Optimal locations of natural archives for $\delta^{18}O$-based NAO reconstructions can be identified with the $\delta^{18}O_p$ sensitivity to the NAO using correlation distribution maps (Baldini et al. 2008), principal component (PC) or canonical correlation analysis (Fischer and Mattey 2012). However, recent studies have shown that migrations of the geographical positions of the NAO dipole relative to those used to define the classical station-based NAO indices (Hurrell 1995; Jones et al. 1997, Fig. 1a) are linked to shifts in the winter temperature and precipitation anomaly patterns in European mid-latitude regions, particularly around 45–50°N (Comas-Bru and McDermott 2014; Raible et al. 2014). Most of these migrations can be rationalised through the concomitant state of the second main atmospheric circulation mode affecting the North Atlantic European region, namely the East Atlantic pattern (EA) (Moore and Renfrew 2012; Moore et al. 2013; Comas-Bru and McDermott 2014). This second mode of sea-level pressure (SLP) variability in the North Atlantic region was first described by Wallace and Gutzler (1981) as anomalously high 500 mb height anomalies over the North Atlantic (near 55°N ; 20–35°W) and low heights over the subtropical Atlantic and eastern Europe when in positive mode. This atmospheric pattern is also prominent

during winter (Barnston and Livezey 1987) and is known to affect precipitation and air temperature patterns over Europe (Rodriguez-Puebla et al. 1998; Comas-Bru and McDermott 2014). Recent studies (Moore and Renfrew 2012) have used an EA index back to 1870 based on SLP data from Valentia Island (Ireland), but this index has also been defined in the literature as the second principal component of regional gridded SLP (Moore et al. 2013; Comas-Bru and McDermott 2014, Fig. 1b).

Migrations of the geographical positions of the NAO dipole mentioned above involve shifts in the southern NAO centre of action toward the southwest when the NAO/EA indices have the same sign, and shifts towards the northeast when the indices have opposing signs (Moore et al. 2013; Comas-Bru and McDermott 2014). As a result, the axis over which the polarity of the NAO climate correlations changes, migrates to higher latitudes when the southern centre of action is closer to the European continent (Comas-Bru and McDermott 2014). Crucially, these migrations of the NAO-winter climate relationship might also affect $\delta^{18}O_p$ patterns, potentially weakening their ability to accurately reflect the NAO at some locations in Europe.

It is well known that a complex set of factors influence $\delta^{18}O_p$ (Yurtsever 1975; Rozanski et al. 1993), but no study has so far addressed the impact of the EA on the spatial $\delta^{18}O_p$ patterns associated with the NAO, or its implications for palaeoclimate reconstructions. Here, for the first time, systematic spatial patterns in $\delta^{18}O_p$ linked to effects of the EA on NAO-$\delta^{18}O_p$ relationships during the observational period are identified. A better understanding of these effects is important to improve the interpretation of natural $\delta^{18}O$ archives in terms of past NAO states in Europe.

2 Data and methods

2.1 $\delta^{18}O$ in precipitation

Precipitation isotopic data ($\delta^{18}O_p$) for the winter months December to February (DJF) were obtained from the International Atomic Energy Agency's Global Network of Isotopes in Precipitation (GNIP; IAEA/WMO 2015), which provides a network of stations over Europe covering the period from March 1960 to December 2013. The 26 stations that have more than 25 complete winters of data and are located in the area 11°W–15°E; 40°N–60°N have been selected (Table 1 and Fig. S1). The stations with the longest records are Vienna (Austria), Groningen (Netherlands) and several stations in Switzerland. A matrix map showing the missing values for all 26 stations is shown in Fig. S2.

In addition, the mean $\delta^{18}O_p$ in winter (DJF) at the surface was also obtained from the output of the isotope-enabled version of the atmospheric general circulation model ECHAM5 (Roeckner et al. 2003, 2006), namely ECHAM5-wiso (Werner et al. 2011), for the N. Atlantic sector (100°W–40°E; 10–80°N) in the period January 1958 to December 2013. For this study, the model has been run at a grid spacing of approximately 1° (T106 spectral mode; comparable to that of Langebroek et al. 2011) in a so-called nudged mode, forced with ECWMF, ERA40 and ERAinterim data (Butzin et al. 2014). As discussed below, annual and seasonal ECHAM5-wiso simulation results are in good agreement with available observations of isotope ratios in precipitation from the GNIP stations (IAEA/WMO 2015) on both global and European scales (Langebroek et al. 2011; Werner et al. 2011).

2.2 Climate variables

Total winter (DJF) precipitation amounts (wPre; mm) and surface air temperatures (wTmp; °C) have been compiled for the North Atlantic European region from the CRU-TS3.1 global observational dataset (Mitchell and Jones 2005) for the period 1959–2009. The horizontal grid interval of this dataset is 0.5° latitude × 0.5° longitude. When available, wPre (mm) and wTmp (°C) have also been obtained at the selected European GNIP stations listed in Table 1. These climate variables are also provided by the ECHAM5-wiso model output (Werner et al. 2011).

2.3 NAO and EA indices

The NAO and EA indices used here are the two leading vectors of the cross-correlation matrix calculated from monthly (December to February) SLP anomalies over a confined Atlantic sector (100°W–40°E; 10–80°N) using ERA40 (Uppala et al. 2005) and ERAinterim (Dee et al. 2011) re-analysis data for the periods December 1957 to February 1979 and December 1979 to February 2013, respectively. This NAO index based on our Principal Component (PC) analysis (Fig. 1a) is similar to the instrumental NAO index calculated as the difference between the normalised SLP over Gibraltar and that over SW Iceland (Jones et al. 1997), updated by the Climate Research Unit of the University of East Anglia (www.cru.uea.ac.uk/~timo/datapages/naoi.htm; $\rho = 0.98$; p value < 0.01; Fig. 1a). Similarly, the PC-based EA index used here is equivalent to that derived from the instrumental December to February SLP data from Valentia Observatory, Ireland ($\rho = 0.81$; p value < 0.01; Fig. 1b). SLP data from this meteorological station was used in previous studies as an instrumental EA index (Moore and Renfrew 2012).

A positive NAO index indicates a strong meridional SLP gradient in the North Atlantic region between the Icelandic low and the Azores high. A positive EA index (consistent with usage by Comas-Bru and McDermott (2014), with

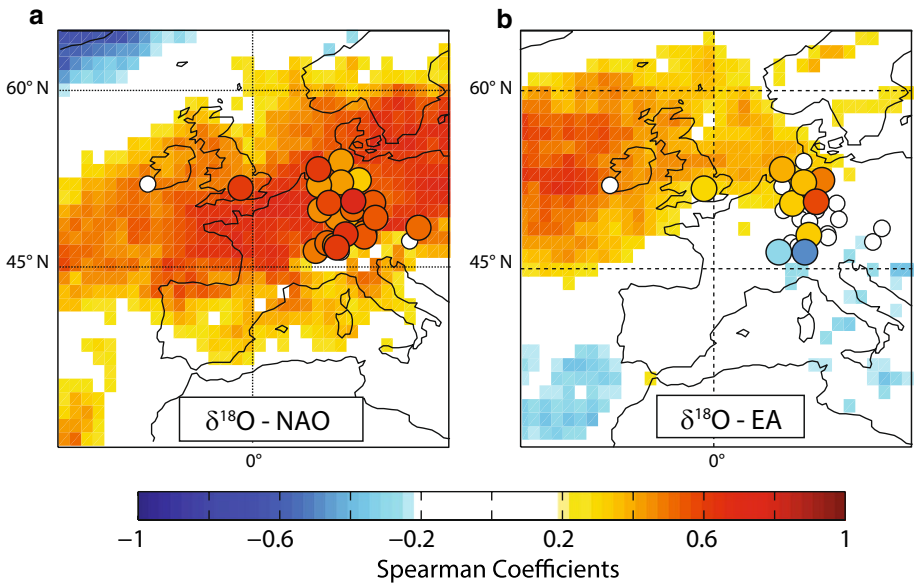

Fig. 2 Spearman correlation coefficients between winter $\delta^{18}O_p$ and **a** NAO; **b** EA using the GNIP data (*coloured circles*; 1961–2013) and the ECHAM5-wiso gridded model output (1959–2013). Significance level at 95 % (*white circles* denote non-significant correlations)

the SLP series from Valentia Observatory (Ireland) used in Moore and Renfrew (2012) and with the original Wallace and Gutzler (1981) definition, but of opposite sign to that of Woollings et al. (2010), Woollings and Blackburn (2012) and Moore et al. (2013)), indicates the presence of positive SLP anomalies over the subtropical North Atlantic during winter, with a centre of action west of Ireland, near 55°N ; 20–35°W. Thus, a positive EA index, as used in this study, is associated with a poleward migration of the North Atlantic jet stream in winter, and the implications of this for observed and modelled $\delta^{18}O_p$ values are discussed below.

2.4 Data selection

Following the approach of previous studies (Moore et al. 2013; Comas-Bru and McDermott 2014), the available monthly $\delta^{18}O_p$ and climate data have been divided in two subsets according to the relative polarity of the NAO and EA indices. The first group (hereafter "EQ") comprises winters with NAO and EA indices of the same sign (n = 36 winters), and corresponds to the subset $(NAO/EA)_S$ defined by Comas-Bru and McDermott (2014). The second group (hereafter "OP") is equivalent to the $(NAO/EA)_O$ subset of Comas-Bru and McDermott (2014), and it includes winters with NAO and EA indices of opposite sign (n = 19 winters).

To aid interpretation, only the NAO > 0 winter sub-set (n = 24) is considered here when calculating absolute differences of $\delta^{18}O_p$, winter surface air temperature and precipitation amount values between OP and EQ winters in Figs. 6 and 7. It is important to note, however, than the same conclusions are valid if only NAO < 0 winters are considered.

3 Results

3.1 Spatial sensitivity of $\delta^{18}O_p$ to atmospheric circulation modes

Consistent with Baldini et al. (2008), broadly positive correlations are observed between winter $\delta^{18}O_p$ and the NAO index for the majority of GNIP stations (Fig. 2a), with non-significant correlations found in the southeast of the study area, and weak correlations observed at the Valentia station (Ireland) and at some stations close to the Baltic Sea. Similar results are obtained using the $\delta^{18}O_p$ modelled with the ECHAM5-wiso model (Fig. 2a). On the other hand, the relationship between $\delta^{18}O_p$ and the EA is much weaker, with few stations showing a significant correlation (Fig. 2b). In this case, $\delta^{18}O_p$ in the southern stations (<∼48°N) is negatively correlated to the EA, whereas positive correlation coefficients occur in the northern locations. A similar change in the sign of the correlation coefficient is observed when the ECHAM-5 wiso model $\delta^{18}O_p$ output is used to calculate the correlations (Fig. 2b), although in most of southern Europe modelled $\delta^{18}O_p$ is not significantly correlated with the EA index.

The spatial $\delta^{18}O_p$-NAO correlation patterns in Europe (Fig. 3a–c) exhibit shifts linked to the relative polarity of the NAO/EA modes that are similar to those reported previously by Comas-Bru and McDermott (2014) for NAO-climate relationships. An important result is that when the NAO and the EA have the same sign (Fig. 3b), the area showing positive $\delta^{18}O_p$-NAO correlations expands over most of north central Europe, whereas when the atmospheric teleconnection patterns have opposite polarity, the positively correlated area is shifted distinctly southwards

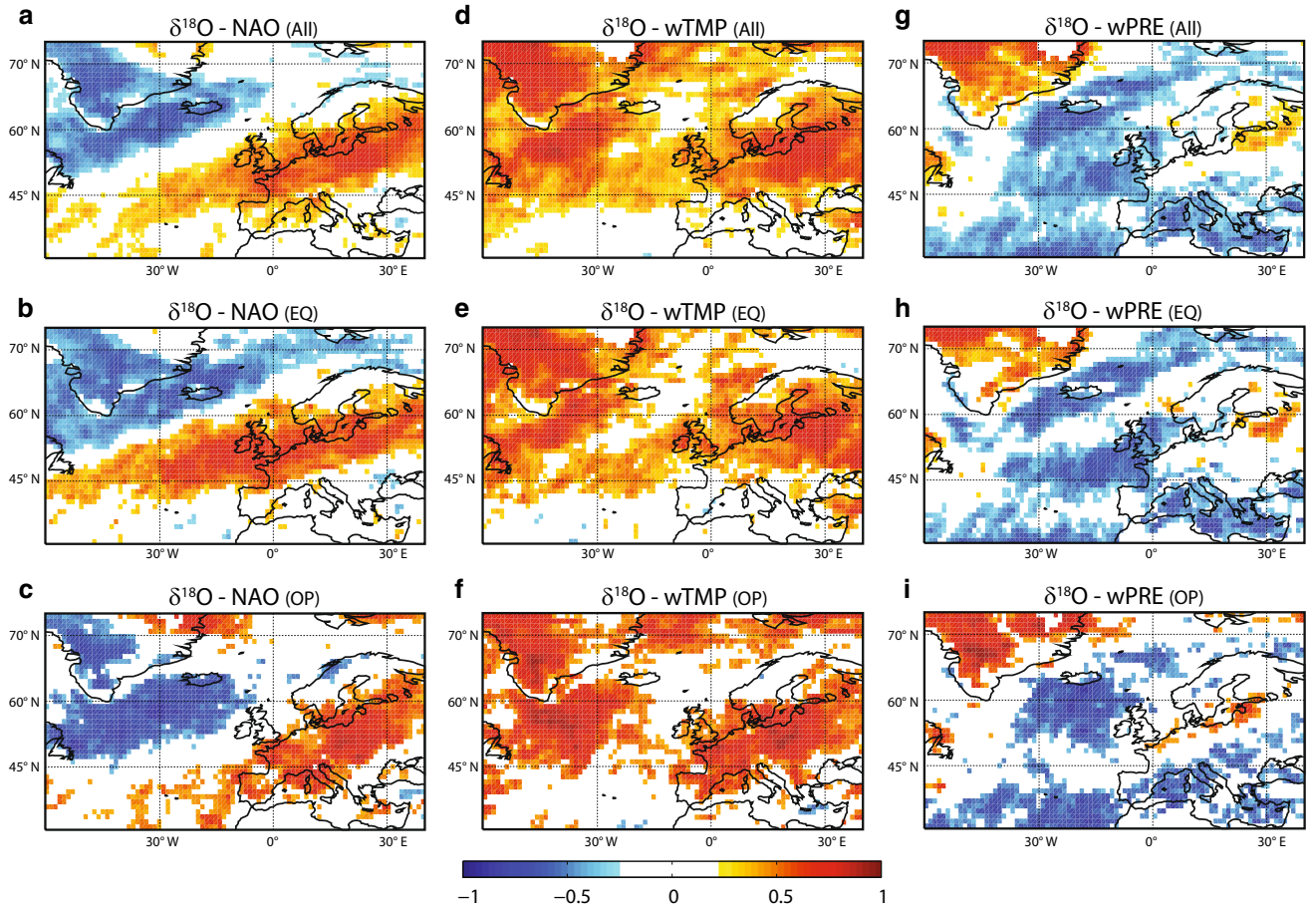

Fig. 3 Spearman correlations between winter $\delta^{18}O_p$ and the NAO index (**a**–**c**); $\delta^{18}O_p$-winter air temperature (wTmp; **d**–**f**) and $\delta^{18}O_p$-winter precipitation amount (wPre; **g**–**i**); for the period 1959–2013 (**a**, **d**, **g**), years with NAO/EA of the same sign (**b**, **e**, **h**; $n = 36$) and years with NAO/EA of opposite sign (**c**, **f**, **i**, $n = 19$). All correlations shown are significant at 95 % level

(Fig. 3c) and the correlation in the Iberian Peninsula improves. Similar patterns are observed in the correlation between $\delta^{18}O_p$ and winter air temperature (wTmp; Fig. 3e, f). In terms of winter precipitation amount (wPre), only the UK and Ireland and some circum-Mediterranean regions are significantly correlated with $\delta^{18}O_p$ (Fig. 3g). However, only in the circum-Mediterranean region the correlations with wPre hold for any combination of NAO and EA polarities (Fig. 3h–i).

To better identify regions that exhibit temporal stationarity in their sensitivity to the NAO in terms of $\delta^{18}O_p$, Fig. 4a illustrates the grid cells where the correlation between $\delta^{18}O_p$-NAO remains significant regardless of the shifts observed in the correlation distribution maps discussed above (Fig. 3b, c). These areas include most of central Europe, the northern coast of the Iberian Peninsula, the southern tip of Sweden and Norway, Iceland and southwest Greenland (Fig. 4a). On the other hand, the relationship between $\delta^{18}O_p$ and wTmp is robust regardless of NAO/EA polarities between 45 and 60°N in Europe, including most of the UK and Ireland, as well as the majority of Greenland (Fig. 4b). Moreover, the correlations between $\delta^{18}O_p$-wPre are robust for the OP and EQ subsets considered here, but are significant at a 95 % level, only in the Italian Peninsula, the Mediterranean islands and parts of Greenland (Fig. 4c).

3.2 Observed and modelled $\delta^{18}O_p$

To assess how the ECHAM5-wiso model output compares with the GNIP observations at specific locations, time series of modelled $\delta^{18}O_p$ have been extracted at the grid-cell locations of four GNIP stations (Fig. 5) selected to cover four distinct regions of Europe: Valentia (S.W. Ireland), Grimsel (Switzerland), Groningen (Netherlands) and Vienna (Austria) (Fig. S1 and Table 1). All stations have more than 38 complete winters of data.

Although an offset to higher $\delta^{18}O_p$ values is modelled in Grimsel, the ECHAM5-wiso model adequately reproduces the temporal $\delta^{18}O_p$ variability observed at the four selected GNIP stations (Fig. 5). Probability

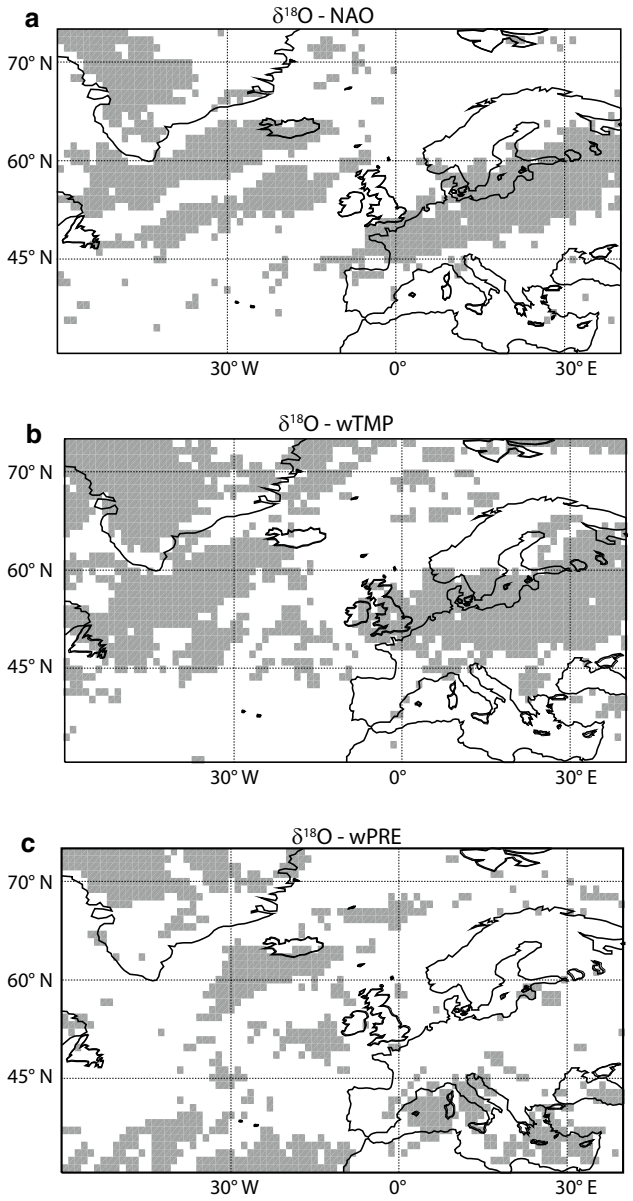

Fig. 4 Map showing the areas where the $\delta^{18}O_p$-NAO (**a**) and the $\delta^{18}O_p$-climate (**b**, **c**) relationships are robust. *Grey* areas indicate the grid cells ($\sim 1° \times 1°$) where Spearman correlations are significant at 95 % for both the OP and EQ subsets.

density functions (PDF) of rainfall $\delta^{18}O_p$ computed for each of these four locations reflect a similar $\delta^{18}O_p$ behaviour during OP and EQ winters in the observations and the ECHAM5-wiso model output (Fig. S3). The $\delta^{18}O_p$ frequency distributions at high latitudes (Valentia and Groningen) show a substantial shift towards higher $\delta^{18}O_p$ during EQ winters (Fig. S3a, b, e, f). On the other hand, a shift towards lower $\delta^{18}O_p$ during EQ winters is observed and modelled at the continental station of Vienna (Fig. S3d, h). Different distributions are evident in the observed and modelled results for the alpine station of Grimsel, however (Fig. S3c, g). While a slight offset towards lower $\delta^{18}O_p$ values during EQ with respect to OP winters is observed in Grimsel (Fig. S3c), the model output shows the opposite behaviour (Fig. S3g) highlighting potential deficiencies in the model output at this grid spacing in regions with steep orography as discussed below. Similar results are also found for other Alpine stations such as Meiringen and Gutannen (not shown).

3.3 Latitudinal response of $\delta^{18}O_p$ to atmospheric circulation mode combinations

To investigate if the North–South trends described for the four selected stations reflect a wider geographical effect at the European GNIP stations listed in Table 1, OP vs. EQ scatterplots of $\delta^{18}O_p$ for NAO > 0 winters are illustrated in Fig. 6a. In addition, the equivalent ECHAM5-wiso $\delta^{18}O_p$ output at those locations is shown (Fig. 6b). Because of the geographical distribution within Europe of the GNIP stations considered in this study (Fig. S1), northerly stations are closer to the coast compared with stations to the south of the area of interest. In Fig. 6, data from the high latitude stations are characterised by higher observed and modelled $\delta^{18}O_p$ values, in contrast to what might be expected if a latitudinal effect only was considered. In essence, the "continental effect" in which progressive distillation of moisture and preferential removal of ^{18}O occurs as storm tracks move eastwards dominates the dataset, with the lower latitude stations in south/central Europe exhibiting lower $\delta^{18}O_p$ values because they are more continental. Our results show that $\delta^{18}O_p$ at low latitude stations is offset to higher values during OP winters compared with EQ winters (Fig. 6), whereas $\delta^{18}O_p$ values at high latitude stations are typically lower during OP winters compared to EQ winters. This is consistent with the PDFs described above for the 4 selected stations (Fig. S3). In contrast, only two stations (Vienna and Graz Universität) show a modelled $\delta^{18}O_p$ higher during OP winters (symbols within a box in Fig. 6b). No clear trends in $\delta^{18}O_p$ between OP and EQ winters are observed or modelled as a function of altitude (Fig. S4).

The absolute differences in several winter parameters between OP and EQ winters at the GNIP stations during NAO > 0 winters, expressed as "$\text{Variable}_{OP} - \text{Variable}_{EQ}$", are shown as a function of latitude in Fig. 7. The trend described above for $\delta^{18}O_p$ (Fig. 6a) is also shown in Fig. 7a, where positive (negative) bars indicate that $\delta^{18}O_p$ is higher (lower) during OP winters than during EQ. The latitudes where $\delta^{18}O_{OP} > \delta^{18}O_{EQ}$ (positive bars in Fig. 7a; <~48°N) correspond to positive differences in air temperature of about 1–1.5 °C (Fig. 7b). On the other hand, at latitudes >50°N , the temperature difference is close to 0.5 °C , with the exception of three stations: Bad Salzuflen (Germany) and Groningen (Netherlands), with

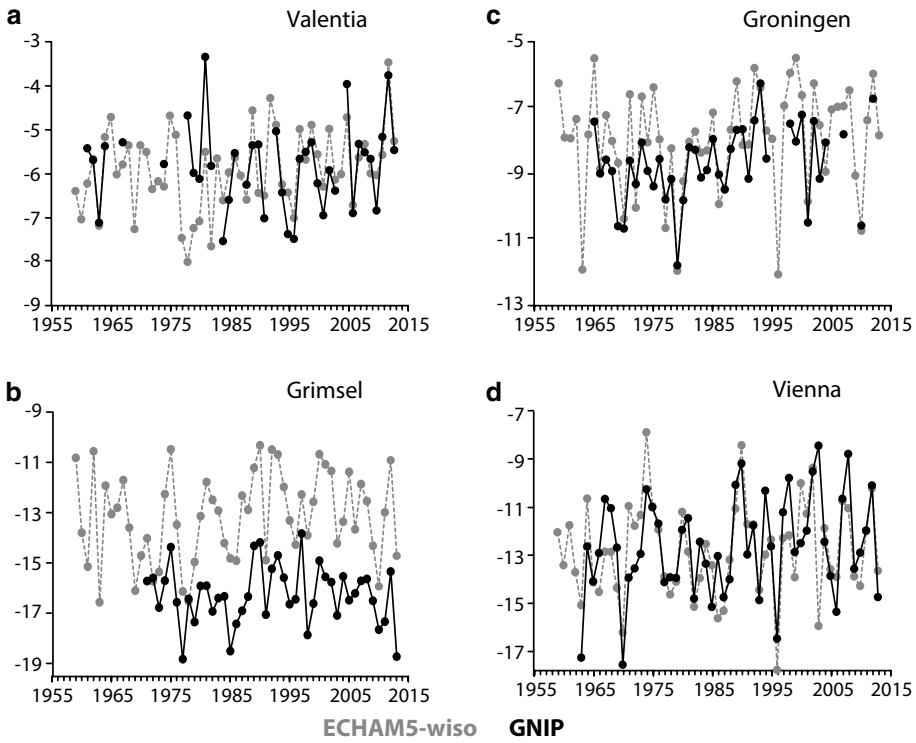

Fig. 5 $\delta^{18}O_p$ time series at the location of four GNIP stations extracted from the ECHAM5-wiso model output (*dashed grey*) and from the GNIP data (*solid black*). The stations are **a** Valentia (Ireland), **b** Groningen (Netherlands), **c** Grimsel (Switzerland) and **d** Vienna (Austria). Their exact locations are shown in Table 1. Each winter mean is ascribed to the year of January (i.e. Dec 1981 to Feb 1982 mean is reported as 1982)

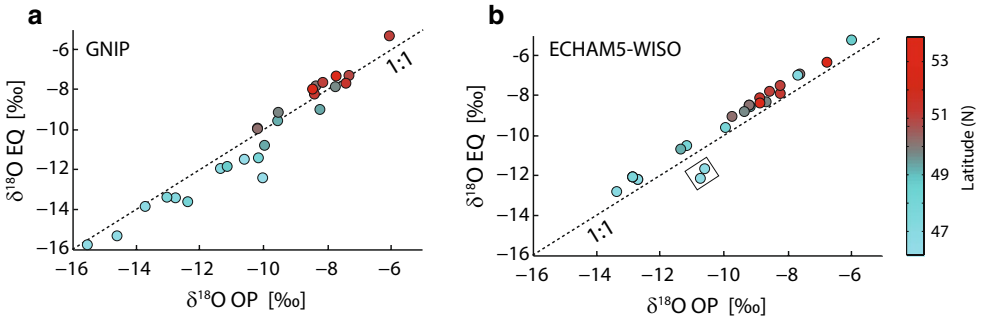

Fig. 6 Scatter plots of $\delta^{18}O_p$ during OP versus EQ winters. **a** Using the GNIP data; **b** using the ECHAM5-wiso model output for the same locations. To aid interpretation, only NAO > 0 winters are considered here. Colour bar refers to the latitude (°N) of each station. Symbols within a *box* in **b** correspond to the modelled output at Vienna and Graz Universität (Austria). See the text for more information on these locations

$wTmp_{OP} - wTmp_{EQ} > 0.5$°C, and Braunschweig (Germany) with $wTmp_{OP} - wTmp_{EQ} < 0$ °C. The differences described above between OP and EQ winters have also been assessed for the N. Atlantic/European region using the ECHAM5-wiso and the CRU-TS3.1 gridded datasets for the periods 1959–2013 and 1959–2009, respectively (Fig. S6). According to the ECHAM5-wiso model output, the largest negative differences in $\delta^{18}O_p$ for OP and EQ winters occur in the North Sea coast and the British Islands, while the most pronounced positive differences are modelled south of the Alps, in northern Italy and Eastern Europe (Fig. S6a). Overall, warmer conditions (about 1–1.5 °C higher) are observed during OP winters over continental Europe (Fig. S6b, d), while wetter conditions occur in Western Europe (Fig. S6c, e).

4 Discussion

Although the temporal correlations between $\delta^{18}O_p$ and the EA index are generally weak in continental Europe for the period 1959–2013 (Fig. 2b), the polarity of this atmospheric mode of winter climate variability in Europe exerts an important influence on the $\delta^{18}O_p$-NAO spatial correlation patterns (Fig. 3a–c). The shifts observed for different NAO/EA scenarios (Fig. 3) are linked to

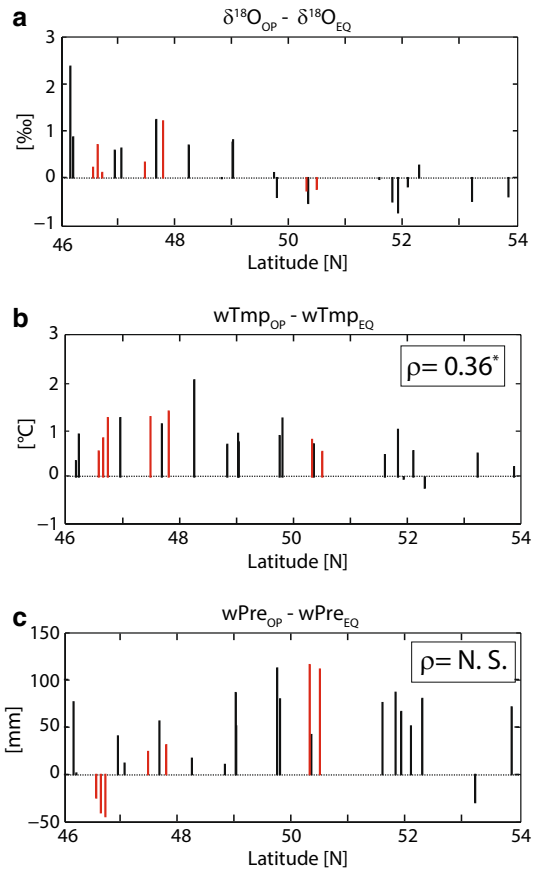

Fig. 7 Differences between OP and EQ winters for a number of winter variables obtained from the GNIP dataset: $\delta^{18}O_p$ (**a**), winter surface air temperature (wTmp; **b**) and winter precipitation amount (wPre; **c**). To aid interpretation, only NAO >0 winters are considered here. Red bars are stations located at elevations >500 m. Rho (ρ) values in **b** and **c** are Spearman correlation coefficients with respect to **a**. The correlation with * is significant at 95 %; the not significant correlation is indicated with N.S

the spatial structure to the SLP dipole in the N. Atlantic region (Comas-Bru and McDermott 2014; Moore et al. 2013) that results in changes of the latitude and speed of the jet stream (Woollings et al. 2010). A positive EA index (Comas-Bru and McDermott 2014) coupled with a positive NAO index results in a northward migration of the jet stream (Woollings and Blackburn 2012). As a result, storm tracks are more likely to enter Europe from the north-west in this condition, having traversed the North Atlantic at higher mean latitudes compared with the south-easterly sourced storm tracks that characterise negative EA conditions. Since only positive NAO conditions are considered for this discussion, positive EA conditions correspond to the EQ winters defined here, and negative EA conditions correspond to the OP winters. Because the northerly stations are closer to the NW coastline of Europe (Fig. S1), storm-tracks arriving predominantly from the north-west (EQ winters) undergo less rainout and Rayleigh distillation, thereby producing rainfall with higher $\delta^{18}O$ values compared with stations in central and southern Europe that are further from the NW European coastline. This effect is clearly observed in the GNIP data (Figs. 6a, 7a) in which $\delta^{18}O_{EQ} > \delta^{18}O_{OP}$ in the high-latitude stations (>48°N), but $\delta^{18}O_{EQ} < \delta^{18}O_{OP}$ in the more continental stations to the south. $\delta^{18}O_{OP}$ values higher than $\delta^{18}O_{EQ}$ values in the south likely reflects rainout from moisture bearing air-masses that have been steered more directly into Europe from the south-west by the southerly-displaced jet stream (Woollings et al. 2010) and that have consequently undergone less isotopic distillation compared with their north-westerly derived counterparts. It is acknowledged that whilst this study groups winters according to their NAO/EA phases, some scatter is observed in $\delta^{18}O_p$ values within a group. This results from the complexity of factors that govern $\delta^{18}O_p$ variability and may imply that the source of the moisture-bearing air-masses could derive from different latitudes in winters that have been grouped together in this study (i.e. OP and EQ winters).

Similar results, although with the zero-line of the $\delta^{18}O_p$ anomalies slightly south of ~48°N, are observed in the ECHAM5-wiso model output (Fig. S6a). This minor disagreement between observed and modelled data could arise from the limitation of the model to reproduce steep orographic effects in the Alps as a consequence of the model grid interval of 1° × 1°. This limitation is indeed reflected in the offset found when comparing GNIP data from three Alpine stations at different altitudes that lie within the same model grid-cell, with the time series extracted from the model output at that location (Fig. S5).

The results presented here have important implications for current efforts to reconstruct past NAO states from $\delta^{18}O$ in natural archives. The non-stationarities between NAO and proxy $\delta^{18}O$ described here have the potential to degrade the $\delta^{18}O$-NAO correlations observed during the calibration period. Consider, for example, a proxy collected in the UK or Ireland covering the instrumental period and an earlier period of interest where the ratio of OP to EQ winters is greater than the value of 0.35 observed during the instrumental period (1959-2013). In this example, the proxy $\delta^{18}O$ -NAO relationship during the period with higher persistence of OP winters, would be weaker than that of the instrumental period, or perhaps even non-significant, as a result of the non-stationarities presented here for UK and Ireland (Fig. 3b, c). Similarly, a stronger $\delta^{18}O$-NAO relationship would be expected for a proxy collected from southern Europe if OP winters were more common than in the calibration period (Fig. 3c).

Hence, collection of natural proxies for NAO reconstruction purposes should be focused on those areas where the correlation between $\delta^{18}O$-NAO is stationary and robust

Table 1 List of GNIP stations used in this study ordered by their latitude in descending order

Station Name	GNIP Code	Country	Lat. (°N)	Lon. (°E)	Alt. (m)	n
CUXHAVEN	1013100	Germany	53.87	8.72	12	33
GRONINGEN	628001	Netherlands	53.23	6.55	1	40
BRAUNSCHWEIG	1034800	Germany	52.30	10.45	88	32
BAD SALZUFLEN	1032500	Germany	52.10	8.73	100	30
VALENTIA (OBSERVATORY)	395300	Ireland	51.93	−10.25	9	38
EMMERICH	1040600	Germany	51.83	6.60	43	31
WALLINGFORD	365302	United Kingdom	51.60	−1.10	48	31
WASSERKUPPE RHOEN	1054400	Germany	50.50	9.95	921	33
KOBLENZ	1051500	Germany	50.35	7.58	97	31
HOF-HOHENSAAS	1068500	Germany	50.32	11.88	567	28
WUERZBURG	1065500	Germany	49.80	9.90	259	34
TRIER	1060900	Germany	49.75	6.70	273	35
REGENSBURG	1077600	Germany	49.03	12.12	377	34
KARLSRUHE	1072700	Germany	49.02	8.38	120	30
STUTTGART (CANNSTATT)	1073900	Germany	48.83	9.20	315	43
VIENNA (HOHE WARTE)	1103500	Austria	48.25	16.37	203	51
HOHENPEISSENBERG	1096200	Germany	47.80	11.02	977	31
KONSTANZ	1092900	Germany	47.68	9.18	447	35
GARMISCH-PARTENKIRCHEN	1096300	Germany	47.48	11.07	720	34
KLAGENFLUGPLATZ	1123100	Austria	47.07	15.45	366	26
BERN	663000	Switzerland	46.95	7.43	511	42
MEIRINGEN	665703	Switzerland	46.73	8.18	632	42
GUTTANNEN	665702	Switzerland	46.65	8.30	1055	43
GRIMSEL	665701	Switzerland	46.57	8.33	1950	43
THONON-LES-BAINS	748501	France	46.22	6.28	385	37
LOCARNO	676000	Switzerland	46.17	8.78	379	29

n indicates the number of complete winters (DJF) available for each station

regardless of the observed changes in the NAO and EA patterns. We identify these areas to be central Europe (north of the Alps), the Cantabrian coast in Northern Spain, the coastal areas surrounding the Baltic sea, Iceland and western Greenland (Fig. 4a). On the other hand, optimal regions for reconstruction of past states of surface air temperature from natural δ^{18}O archives include the areas surrounding the North and the Baltic Sea, as well as some regions in central Europe and most of inland Greenland (4b). Similarly, if the aim is to reconstruct precipitation amounts using a proxy for $\delta^{18}O_p$, only Italy and a few coastal sites in the circum-Mediterranean region would be suitable (4c).

5 Conclusions

Ideally, $\delta^{18}O_p$-NAO relationships should remain stationary through time in order to use δ^{18}O variations in natural archives as proxies to reconstruct past NAO states. Identification of regions subject to non-stationarities of the $\delta^{18}O_p$-NAO relationship is crucial so that resources can be focused in the areas least affected by such non-stationarities.

Here we show that it can be anticipated that natural δ^{18}O archives will exhibit different degrees of stationarity in their $\delta^{18}O_p$ response to the NAO in many regions of Europe simply as a function of temporal changes in the EA pattern. This observation can be rationalised through changes in the SLP structure in the N. Atlantic region as a result of the concomitant states of the NAO and EA patterns, which affect the trajectories of the air-masses carrying moisture onto Europe and ultimately the $\delta^{18}O_p$ signal. Proxy calibration (an overlapping period with instrumental data) could be compromised or biased by different NAO/EA combinations within the calibration dataset. Depending on the proxy location, the slopes of $\delta^{18}O_{proxy}$/climate variable data trends could be affected by different persistence patterns of the NAO and EA modes within the instrumental calibration period, compared with that expected over longer timescales of the proxy record. We have identified regions where $\delta^{18}O_p$ shows a robust stationary relationship with the

NAO regardless of the concomitant state of the EA during the instrumental period. These regions are central Europe (north of the Alps), the northern coast of the Iberian Peninsula, Iceland and west Greenland (Fig. 4).

Acknowledgments We would like to thank Met Éireann (Irish Meteorological Service) for providing the sea-level pressure data from Valentia Observatory (Ireland). The authors are grateful to the journal editor, Dr. Susanna Corti, and two anonymous reviewers for their insightful comments.

References

Baldini LM, McDermott F, Foley AM, Baldini JUL (2008) Spatial variability in the European winter precipitation δ^{18}O-NAO relationship: Implications for reconstructing NAO-mode climate variability in the Holocene. Geophys Res Lett 35:L04709. doi:10.1029/2007GL032027

Baldini LM, McDermott F, Baldini JUL, Fischer MJ, Möllhoff M (2010) An investigation of the controls on Irish precipitation δ^{18}O values on monthly and event timescales. Clim Dyn 35(6):977–993. doi:10.1007/s00382-010-0774-6

Barnston AG, Livezey RE (1987) Classification, seasonality and persistence of low-frequency atmospheric circulation patterns. Mon Weather Rev 115:1083–1126

Butzin M, Werner M, Masson-Delmotte V, Risi C, Frankenberg C, Gribanov K, Jouzel J, Zakharov VI (2014) Variations of oxygen-18 in West Siberian precipitation during the last 50 years. Atmos Chem Phys 14(11):5853–5869. doi:10.5194/acp-14-5853-2014

Comas-Bru L, McDermott F (2014) Impacts of the EA and SCA patterns on the European twentieth century NAOwinter climate relationship. Q J R Meteorol Soc 140(679):354–363. doi:10.1002/qj.2158

Compo GP, Whitaker JS, Sardeshmukh PD, Matsui N, Allan RJ, Yin X, Gleason BE, Vose RS, Rutledge G, Bessemoulin P, Brönnimann S, Brunet M, Crouthamel RI, Grant AN, Groisman PY, Jones PD, Kruk MC, Kruger AC, Marshall GJ, Maugeri M, Mok HY, Nordli Ø, Ross TF, Trigo RM, Wang XL, Woodruff SD, Worley SJ (2011) The twentieth century reanalysis project. Q J R Meteorol Soc 137(654):1–28. doi:10.1002/qj.776

Dee DP, Uppala SM, Simmons AJ, Berrisford P, Poli P, Kobayashi S, Andrae U, Balmaseda MA, Balsamo G, Bauer P, Bechtold P, Beljaars ACM, van de Berg L, Bidlot J, Bormann N, Delsol C, Dragani R, Fuentes M, Geer AJ, Haimberger L, Healy SB, Hersbach H, Hólm EV, Isaksen L, Kållberg P, Köhler M, Matricardi M, McNally AP, Monge-Sanz BM, Morcrette J-J, Park B-K, Peubey C, de Rosnay P, Tavolato C, Thépaut J-N, Vitart F (2011) The ERA-interim reanalysis: configuration and performance of the data assimilation system. Q J R Meteorol Soc 137(656):553–597. doi:10.1002/qj.828

Feng X, Reddington AL, Faiia AM, Posmentier ES, Shu Y, Xu X (2007) The changes in North American atmospheric circulation patterns indicated by wood cellulose. Geology 35(2):163–166. doi:10.1130/g22884a.1

Fischer MJ, Mattey D (2012) Climate variability and precipitation isotope relationships in the Mediterranean region. J Geophys Res: Atmos 117(D20):D20112. doi:10.1029/2012jd018010

Friedman I, Harris JM, Smith GI, Johnson CA (2002) Stable isotope composition of waters in the Great Basin, United States 1. Air-mass trajectories. J Geophys Res: Atmos 107(D19):4400. doi:10.1029/2001jd000565

Hurrell JW, Kushnir Y, Ottersen G, Visbeck M (2003) An overview of the North Atlantic Oscillation. In: The North Atlantic Oscillation: climatic significance and environmental impact. Geophysical Monograph Series, vol 134. American Geophysical Union (AGU), Washington, pp 1–35. doi:10.1029/GM134

Hurrell JW (1995) Decadal trends in the North Atlantic oscillation: regional temperatures and precipitation. Science 269:676–679. doi:10.1126/science.269.5224.676

IAEA/WMO (2015) Global Network of Isotopes in Precipitation. The GNIP Database. http://www.iaea.org/water. Accessed 23 June 2015

Jones PD, Jonsson T, Wheeler D (1997) Extension to the North Atlantic Oscillation using early instrumental pressure observations from Gibraltar and south-west Iceland. Int J Climatol 17:1433–1450

Jones PD, Briffa KR, Osborn TJ, Lough JM, van Ommen TD, Vinther BM, Luterbacher J, Wahl ER, Zwiers FW, Mann ME, Schmidt GA, Ammann CM, Buckley BM, Cobb KM, Esper J, Goosse H, Graham N, Jansen E, Kiefer T, Kull C, Kuettel M, Mosley-Thompson E, Overpeck JT, Riedwyl N, Schulz M, Tudhope AW, Villalba R, Wanner H, Wolff E, Xoplaki E (2009) High-resolution palaeoclimatology of the last millennium: a review of current status and future prospects. Holocene 19(1):3–49. doi:10.1177/0959683608098952

Langebroek PM, Werner M, Lohmann G (2011) Climate information imprinted in oxygen-isotopic composition of precipitation in Europe. Earth Planet Sci Lett 311(1–2):144–154. doi:10.1016/j.epsl.2011.08.049

Lawrence JR, Gedzelman SD, White JWC, Smiley D, Lazov P (1982) Storm trajectories in eastern US D/H isotopic composition of precipitation. Nature 296(5858):638–640. doi:10.1038/296638a0

Liu Z, Bowen GJ, Welker JM (2010) Atmospheric circulation is reflected in precipitation isotope gradients over the conterminous United States. J Geophys Res: Atmos 115(D22):D22120. doi:10.1029/2010jd014175

Liu Z, Bowen GJ, Welker JM, Yoshimura K (2013) Winter precipitation isotope slopes of the contiguous USA and their relationship to the Pacific/North American (PNA) pattern. Clim Dyn 41(2):403–420. doi:10.1007/s00382-012-1548-0

Luterbacher J, Xoplaki E, Dietrich D, Rickli R, Jacobeit J, Beck C, Gyalistras D, Schmutz C, Wanner H (2002) Reconstruction of sea level pressure fields over the Eastern North Atlantic and Europe back to 1500. Clim Dyn 18(7):545–561. doi:10.1007/s00382-001-0196-6

Mitchell TD, Jones PD (2005) An improved method for constructing a database of monthly climate observations and associated high-resolution grids. Int J Climatol 25:693–712. doi:10.1002/joc.1181

Moore GWK, Renfrew IA, Pickart RS (2013) Multidecadal mobility of the North Atlantic Oscillation. J Clim 26(8):2453–2466. doi:10.1175/jcli-d-12-00023.1

Moore GWK, Renfrew IA (2012) Cold European winters: interplay between the NAO and the East Atlantic mode. Atmos Sci Lett 13:1–8. doi:10.10025/asl.356

Raible CC, Lehner F, González-Rouco JF, Fernández-Donado L (2014) Changing correlation structures of the northern hemisphere atmospheric circulation from 1000 to 2100 AD. Clim Past 10(2):537–550. doi:10.5194/cp-10-537-2014

Rodriguez-Puebla C, Encinas AH, Nieto S, Garmeinda J (1998) Spatial and temporal patterns of annual precipitation variability over the Iberian peninsula. Int J Climatol 18:299–316. doi:10.1002/(SICI)1097-0088(19980315)18:3<299::AID-JOC247>3.0.CO;2-L

Roeckner E, Bäuml G, Bonaventura L, Borokopf R, Esch M, Giorgetta M, Hagemann S, Kirchner I, Kornblueh L, Manzini E, Rhodin A, Schlese U, Schulzweida U, Tompkins A (2003) The atmospheric general circulation model ECHAM5. PART 1: Model description. Report no 349. Max-Plank-Insitut für Meteorologie, Hamburg

Roeckner E, Brokopf R, Esch M, Giorgetta M, Hagemann S, Kornblueh L, Manzini E, Schlese U, Schulzweida U (2006) Sensitivity of simulated climate to horizontal and vertical resolution in the ECHAM5 atmosphere model. J Clim 19(16):3771–3791. doi:10.1175/JCLI3824.1

Rozanski K, Araguás-Araguás L, Gonfiantini R (1993) Isotopic patterns in modern global precipitation. In: Geophysical Monograph 78. Climate Change in Continental Isotopic Records 1-36. AGU, Washington, DC, doi:10.1029/GM078p0001

Smith MA, Hollander DJ (1999) Historical linkage between atmospheric circulation patterns and the oxygen isotopic record of sedimentary carbonates from Lake Mendota, Wisconsin, USA. Geology 27(7):589–592. doi:10.1130/0091-7613(1999)027<0589:hlbacp>2.3.co;2

Trouet V, Esper J, Graham NE, Baker A, Scourse JD, Frank DC (2009) Persistent positive North Atlantic Oscillation mode dominated the medieval climate anomaly. Science 324:78–80. doi:10.1126/science.1166349

Uppala SM, Kållberg PW, Simmons AJ, Andrae U, da Costa Bechtold V, Fiorino M, Gibson JK, Haseler J, Hernandez A, Kelly GA, Li X, Onogi K, Saarinen S, Sokka N, Allan RP, Andersson E, Arpe K, Balmaseda MA, Beljaars ACM, Van De Berg L, Bidlot J, Bormann N, Caires S, Chevallier F, Dethof A, Dragosavac M, Fisher M, Fuentes M, Hagemann S, Hólm E, Hoskins BJ, Isaksen L, Janssen PAEM, Jenne R, Mcnally AP, Mahfouf J-F, Morcrette J-J, Rayner NA, Saunders RW, Simon P, Sterl A, Trenberth KE, Untch A, Vasiljevic D, Viterbo P, Woollen J (2005) The ERA-40 re-analysis. Q J R Meteorol Soc 131(612):2961–3012. doi:10.1256/qj.04.176

Wallace JM, Gutzler DS (1981) Teleconnections in the geopotential height field during the Northern Hemisphere winter. Mon Weather Rev 109:784–812. doi:10.1175/1520-0493(1981)109<0784:TITGHF>2.0.CO;2

Wanner H, Brönnimann S, Casty C, Gyalistras D, Lutherbacher J, Schmutz CJ, Stephenson DB, Xoplaki E (2001) North Atlantic Oscillation: concepts and studies. Surv Geophys 22:321–382. doi:10.1023/A:1014217317898

Werner M, Langebroek PM, Carlsen T, Herold M, Lohmann G (2011) Stable water isotopes in the ECHAM5 general circulation model: toward high-resolution isotope modeling on a global scale. J Geophys Res-Atmos 116:14. doi:10.1029/2011jd015681

Woollings T, Hannachi AL, Hoskins B (2010) Variability of the North Atlantic eddy-driven jet stream. Q J R Meteorol Soc 136(649):856–868. doi:10.1002/qj.625

Woollings T, Blackburn M (2012) The North Atlantic jet stream under climate change and its relation to the NAO and EA patterns. J Clim 25(3):886–902. doi:10.1175/jcli-d-11-00087.1

Yurtsever Y (1975) Worldwide survey of isotopes in precipitation. IAEA report, Vienna